

Status report of the NuMoon experiment.

O. Scholten^a S. Buitink^b J. Bacelar^c R. Braun^d
 A.G. de Bruyn^{e,f} H. Falcke^b K. Singh^a B. Stappers^g
 R.G. Strom^{h,f} R. al Yahyaoui^a

^a*Kernfysisch Versneller Instituut, University of Groningen, 9747 AA, Groningen, The Netherlands*

^b*Department of Astrophysics, IMAPP, Radboud University, 6500 GL Nijmegen, The Netherlands*

^c*ASML Netherlands BV, P.O.Box 324, 5500 AH Veldhoven, The Netherlands*

^d*CSIRO-ATNF, P.O.Box 76, Epping NSW 1710, Australia*

^e*Kapteyn Institute, University of Groningen, 9747 AA, Groningen, The Netherlands*

^f*ASTRON, 7990 AA Dwingeloo, The Netherlands*

^g*School of Physics & Astronomy, Alan Turing Building, Univ. of Manchester, Manchester, M13 9PL*

^h*Astronomical Institute 'A. Pannekoek', University of Amsterdam, 1098 SJ, The Netherlands*

Abstract

We show that at wavelengths comparable to the length of the shower produced by an Ultra-High Energy cosmic ray or neutrino, radio signals are an extremely efficient way to detect these particles. First results are presented of an analysis of 20 hours of observation data for NuMoon project using the Westerbork Synthesis Radio Telescope to search for short radio pulses from the Moon. A limit on the neutrino flux is set that is a factor four better than the current one (based on FORTE).

Key words: Ultra-High Energy Cosmic Ray, UHE Neutrinos, radio waves

PACS: 95.55.Vj, 95.55.Jz, 95.75.Wx, 95.85.Ry, 98.70.Rz

Email address: scholten@kvi.nl (O. Scholten).

2 Introduction

An efficient method to determine the fluxes of Ultra High Energy (UHE) particles is through the production of coherent radio waves [1] when an UHE particle hits the moon. At sufficiently high energy the pulses are detectable at Earth with radio telescopes, an idea first proposed by Dagkesamanskii and Zheleznyk [2]. Several experiments have since been performed [3,4]. These experiments have looked for radiation near the frequency where the intensity is expected to reach its maximum. Since the typical lateral size of a shower is of the order of 10 cm the peak frequency is of the order of 3 GHz.

We propose [5] to look for the radio waves at considerably lower frequencies where the wavelength of the radiation is comparable in magnitude to the typical longitudinal size of showers. As discussed in Section 3 the lower intensity of the emitted radiation is compensated by an increase in detection efficiency due to the near isotropic emission of coherent radiation, resulting in an increase of sensitivity by several orders of magnitude. In Section 4 we discuss the on-going observations made for the NuMoon project with the Westerbork Synthesis Radio-Telescope array (WSRT) and the neutrino-flux limit which has been determined from 20 hours observation time.

3 Radio Emission

The intensity of radio emission from a hadronic shower with energy E_s can be parameterized as given in Ref. [5]. The angle at which the intensity of the radiation reaches a maximum, the Čerenkov angle, is related to the index of refraction (n) of the medium, $\cos\theta_c = 1/n$. Since the angular spread of the intensity is crucial for our considerations, we have derived analytic formulas for a “block” and a “sine” shower profile [5,6], curves labeled respectively ‘b’ and ‘s’ in Fig. 1. For a shower of 10^{20} eV It is seen that at 2.2 GHz the simple exponential form [4,7,8] approximates well the analytic forms. At 100 MHz (right hand panel of Fig. 1) the analytic expressions all give similar results differing from the phenomenological exponential parameterization. The reason for this difference lies mainly in the pre-factor $\sin^2\theta$ which accounts for the radiation being polarized parallel to the shower, not allowing for emission at 0° and 180° .

Cosmic-ray-induced showers occur effectively at the lunar surface. For neutrino-induced showers an energy-dependent mean free path has been used. The

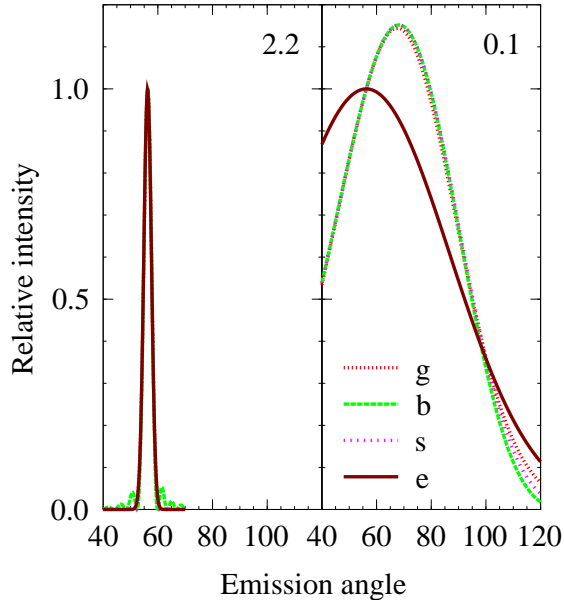


Fig. 1. The angular spread around the Čerenkov angle for different shower-profile functions (see text) are compared to the parametrization used in this work. The left (right) hand displays the results for 2.2 GHz (100MHz) respectively.

attenuation length for the radiated power in the regolith is set at $\lambda_r = (9/\nu[\text{GHz}])$ m. A crucial point in the simulation is the refraction of radio waves at the lunar surface [8]. The emitted radiation at high frequencies where the Čerenkov cone is rather narrow will be severely diminished due to internal reflection at the surface. The major advantage of going to lower frequencies is that the angular spreading increases, allowing the radiation to penetrate the lunar surface. With decreasing frequency the intensity of the emitted radiation decreases, however, the intensity increases with increasing particle energy. The net effect is that at sufficiently-high shower energies the aforementioned effect of increased spreading is far more important, resulting in a strong increase in the detection probability, see Fig. 2. An additional advantage of using lower frequencies is that the sensitivity of the model simulations to large- or small-scale surface roughness is diminished since the angular spread is already large. This is in contrast to high frequencies where most of the radiation is internally reflected when surface roughness is ignored. The thickness of the regolith is about 10–100 m and known to vary over the lunar surface. There is a (probably smooth) transition to solid rock, for which the density is about twice that of the regolith. The crust appears to be homogeneous in composition up to depths of about 20 km where there is a seismic discontinuity [9]. Pure rock and regolith have been simulated and found to give very similar detection limits for low frequencies [5].

4 WSRT observations

The Westerbork Radio Synthesis Telescope (WSRT) is an array telescope consisting of 14 parabolic telescopes of 25 m on a 2.7 km east-west line. The

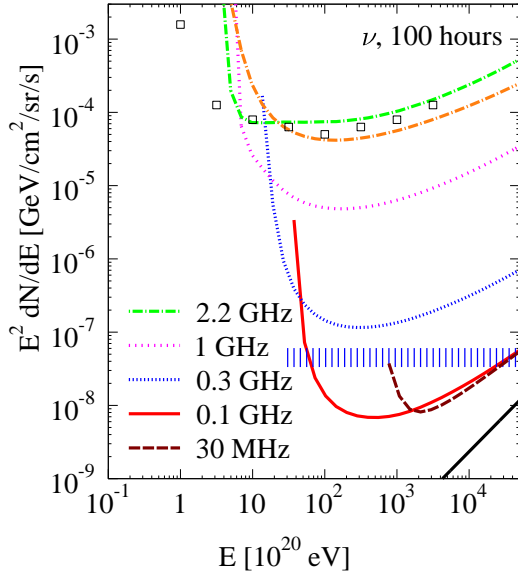


Fig. 2. Flux limits (assuming a null observation) for neutrinos as can be determined in a 100 hour observation. In the curves for $\nu = 30$ MHz a ten fold higher detection threshold is used, corresponding to the higher sky temperature at this frequency. The thick black line corresponds to the best possible limit (vanishing detection threshold). The open squares for the neutrino flux are the limits determined from the GLUE experiment [4].

NuMoon experiment uses the Low Frequency Front Ends (LFFEs) which cover the frequency range 115–180 MHz and record full polarization data. For our observations we use the Pulsar Machine II backend [10], which can record 8 Nyquist sampled bands with a bandwidth of 20 MHz each (40 MHz sampling frequency). We use two beams of 4 bands each, centered around 123, 137, 151, and 165 MHz. The two beams are aimed at different sides of the Moon, each covering about one third of the lunar surface. A real lunar Cherenkov pulse should only be visible in only one of the two beams. Because of overlap the total bandwidth per beam is 65 MHz.

In the first pass a rough search for pulses is performed to retain about 1% of the data, stored permanently. The procedure involves the following steps [16]:

- (1) The raw data is read in blocks of 20 000 time bins each and Fourier transformed to excise narrow-band radio-frequency interference (RFI). The left panel in Fig. 3 shows the frequency spectrum for band centered around 165 MHz of 10 seconds of data before RFI removal. The right hand side shows the effects of RFI removal.
- (2) The data is transformed back to the time domain after a de-dispersion is performed, based on the slanted total electron content (STEC) of the ionosphere. This corrects for the dispersion of signals coming from the Moon.
- (3) The pulses of interest have a width smaller than the bin size (25 ns) and should thus be sharp in the de-dispersed data. However a Nyquist-sampled, bandwidth limited, pulse can be three time-samples long. In addition a mismatch in the STEC value used for de-dispersion will further broaden the pulse. We define the value $P5$ as the power integrated over 5 time bins and 2 polarizations, normalized to the average value of this

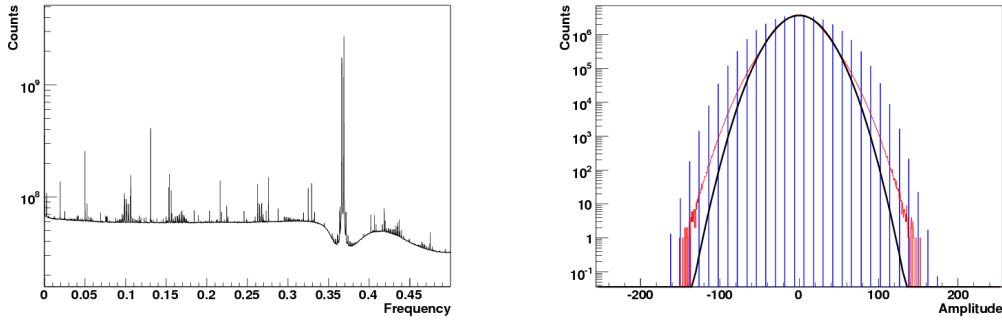


Fig. 3. Left: Typical frequency spectrum of 10 seconds of data before RFI reduction. The x-axis shows arbitrary units. Right: Typical results of RFI reduction. The number of counts per amplitude is plotted for the raw data (blue) and the data after RFI reduction (red). The black line is a Gaussian fit to the data after RFI reduction.

integration, $P5 = P5_x + P5_y$ with $P5_i = \sum_{5 \text{ bins}} P_i / \left\langle \sum_{5 \text{ bins}} P_i \right\rangle$ where the averaging is done per block.

- (4) A peak search is carried out, where we use a trigger condition of a $P5$ value of 2.5 in all four frequency bands. A time difference between the peaks in the different frequency bands is allowed to account for a possible error in the STEC value used in de-dispersion. For each trigger the data blocks in which the pulses are found are stored for postprocessing.

In the second pass, further cuts are applied to the data. Pulses of a width exceeding 8 bins are rejected, as well as pulses that coincide with a regular timer pulse.

5 Results

Presently, 10 hours and 40 minutes of single beam data have been accumulated. Fig. 4 shows the distribution of $P5$ values with no cuts applied (black line), a cut on pulse width (red line) and a cut on the timing signal (green line). For pure Gaussian noise the number of expected triggers is of the order of unity at $P5 \approx 14$.

The highest value surviving this cut is $P5 = 25$. For the WSRT the system noise at low frequencies is $F_{noise} = 600$ Jy per polarization channel, so $P5 = 1$ corresponds to 6000 Jy, giving a detection threshold of ~ 38 kJy. Fig. 5 shows the limit on the neutrino flux that is obtained with the current 20 hours of data based on this detection threshold. Also shown is the limit that can be achieved with a 100 hour observation period. The current limits in the UHE

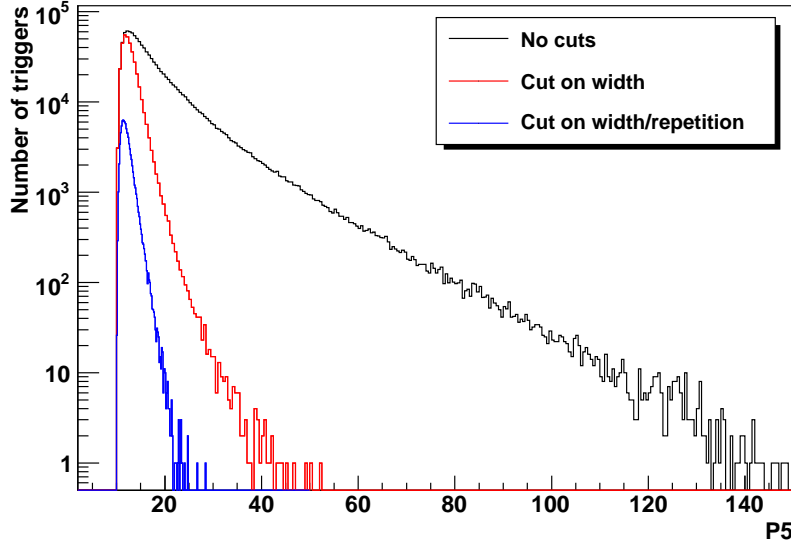


Fig. 4. Number of triggers plotted against the P5 value for different cuts.

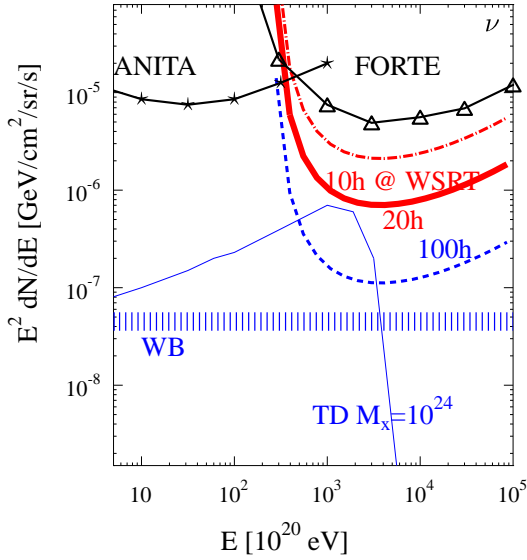


Fig. 5. Neutrino flux limit currently established with 20 hours of WSRT data and the limit that will be achieved with 100 hours. Limits from ANITA and FORTE are included in the plot as well as the Waxman-Bahcall flux and a TD model prediction.

region are established by ANITA [17] and FORTE [6]. Two model predictions are plotted: the Waxman-Bahcall limit [14] and a top-down model [15] for exotic particles of mass $M_X = 10^{24}$ eV.

6 Discussion

We observe at a frequency window that offers an optimal sensitivity to lunar pulses. Because of the large spread in emission angle, we expect no systematic effect from surface irregularities. The detection efficiency is also largely inde-

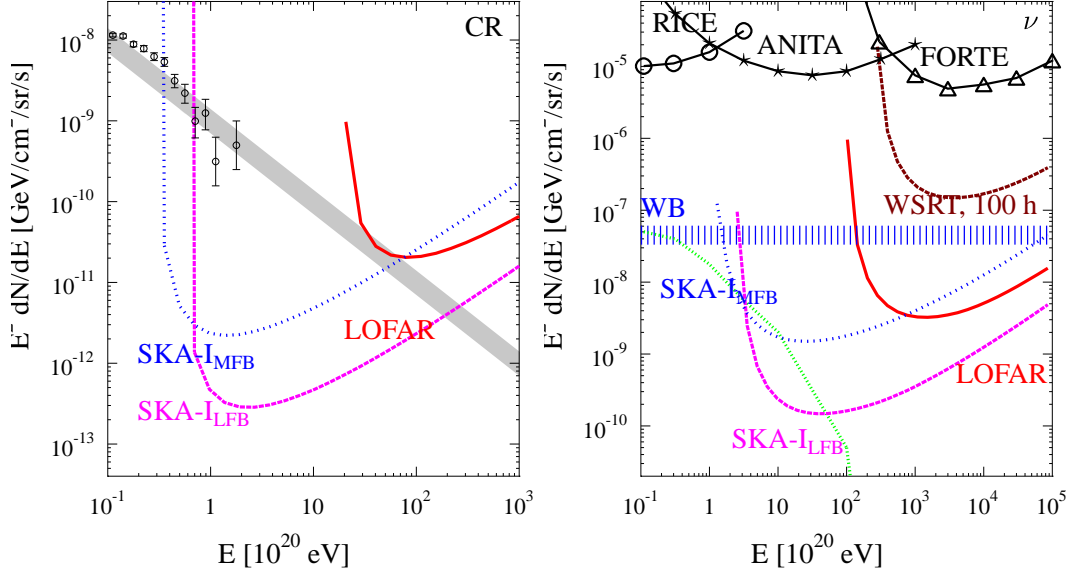


Fig. 6. Limits on UHE neutrino flux (left) and cosmic ray flux (right) that can be established with LOFAR and SKA.

pendent from details in the structure of the (sub-)regolith [5]. With about 100 hours of observation data we will be able to put a limit on the UHE neutrino flux which is about an order of magnitude lower than the current FORTE limit (assuming no detections). This limit would rule out a subset of TD models (see Fig. 5).

The next phase in the NuMoon project will be to use LOFAR, the Low Frequency Array, that is under construction in the Netherlands. LOFAR is a network of low frequency omni-directional radio antennas communicating over a fiber optics network. Half of the stations are located inside the 2 km \times 2 km core with a total collecting area of ~ 0.05 km 2 . Multiple beams can be formed to cover the surface of the Moon, resulting in a sensitivity that is about 25 times better than the WSRT. Fig. 6 shows the sensitivity that will be achieved with 30 days of observation time with LOFAR for UHE cosmic rays (left panel) and neutrinos (right panel).

Other lunar Cherenkov observations will be carried out at the Australia Telescope Compact Array (ATCA) [18] consisting of six 22 m dishes. The array is currently undergoing an upgrade to be able to measure with a bandwidth of 2 GHz. The upgrade is projected to be finished in 2009.

Eventually, the best sensitivity will be achieved with the Square Kilometer Array [19] (SKA), planned to be completed in 2020. The Australian SKA Pathfinder (ASKAP) is expected to be operational around 2011. In Fig. 6 the expected sensitivity of SKA is plotted for observations in the low frequency band (70–200 MHz) and the middle frequency band (200–300 MHz).

This work was performed as part of the research programs of the Stichting voor Fundamenteel Onderzoek der Materie (FOM) and of ASTRON, both with financial support from the Nederlandse Organisatie voor Wetenschappelijk Onderzoek (NWO).

References

- [1] G. A. Askaryan, Sov. Phys. JETP **14**, 441 (1962); **21**, 658 (1965).
- [2] R. D. Dagkesamanskii and I.M. Zheleznyk, Sov. Phys. JETP **50**, 233 (1989).
- [3] T. H. Hankins, R. D. Ekers, and J. D. OSullivan, Mon. Not. R. Astron. Soc. **283**, 1027 (1996).
- [4] P. Gorham et al., Phys. Rev. Lett. **93**, 41101 (2004).
- [5] O. Scholten et al., Astropart. Phys. **26**, 219 (2006).
- [6] N.G. Lehtinen, P.W. Gorham, A.R. Jacobson and R.A. Roussel-Dupre, Phys. Rev. D **69**, 013008 (2004).
- [7] J. Alvarez-Muñiz, R. A. Vazquez, and E. Zas, Phys. Rev. D **61**, 23001 (99).
- [8] E. Zas, F. Halzen, and T. Stanev, Phys. Rev. D **45**, 362 (1992); J. Alvarez-Muñiz and E. Zas, Phys. Lett. B **411**, 218 (1997).
- [9] M.A. Wieczorek and M.T. Zuber, Geophys. Res. Lett., **28**, 4023 (2001).
- [10] R. Karuppusamy, B. Stappers, W. van Straten, astro-ph/0802.2245v1
- [11] J. Alvarez-Muñiz and E. Zas, Phys. Lett. B **434**, 396 (1998).
- [12] Tokonatsu Yamamoto et al., Proc. of the 30th ICRC, Merida, Mexico, 2007, #318; astro-ph/07072638v1.
- [13] J.D. Bregman, Proceedings of the SPIE, **4015**, 19 (2000); H. Butcher, Proceedings of the SPIE, **5489**, 537 (2004); see also <http://www.lofar.org/>.
- [14] J. Bahcall and E. Waxman, Phys. Rev. D **64**, 64 (2001).
- [15] R.J. Protheroe, T. Stanev, Phys. Rev. Lett. **77**, 3708 (1996).
- [16] S. Buitink, proceedings Blois meeting.
- [17] S.W. Barwick et al., Phys. Rev. Lett. **96**, 171101 (2006).
- [18] C.W. James and R.J. Protheroe, astro-ph/08023562v1
- [19] <http://www.skatelescope.org/> SKA website (2008)